Modeling the Hydrogeochemical Transport of Radionuclides through Engineered Barriers System in the Proposed LLW Disposal Site of Taiwan - 12082

Wen-Sheng Lin[1], Chen-Wuing Liu[2], Jui-Hsuan Tsao[2], Ming-Hsu Li[3]

[1]Hydrotech Research Institute, National Taiwan University, Taipei, Taiwan(R.O.C.)

[2]Department of Bioenvironmental Systems Engineering, National Taiwan University, Taipei, Taiwan (R.O.C.)

[3]Institute of Hydrological and Oceanic Sciences, National Central University, Jhongli, Taiwan (R.O.C.)

ABSTRACT

A proposed site for final disposal of low-level radioactive waste located in Daren Township of Taitung County along the southeastern coast has been on the selected list in Taiwan. The geology of the Daren site consists of argillite and meta-sedimentary rocks. A mined cavern design with a tunnel system of 500 m below the surface is proposed. Concrete is used as the main confinement material for the engineered barrier. To investigate the hydrogeochemical transport of radionuclides through engineered barriers system, HYDROGEOCHEM5.0 model was applied to simulate the complex chemical interactions among radionuclides, the cement minerals of the concrete, groundwater flow, and transport in the proposed site. The simulation results showed that the engineered barriers system with the side ditch efficiently drained the ground water and lowered the concentration of the concrete degradation induced species (e.g., hydrogen ion, sulfate, and chloride). The velocity of groundwater observed at side ditch gradually decreased with time due to the fouling of pore space by the mineral formation of ettringite and thaumasite. The short half-life of Co-60, Sr-90 and Cs-137 significantly reduced the concentrations, whereas the long half-life of I-129(1.57×10^7 years) and Am-241(432 years) remain stable concentrations at the interface of waste canister and concrete barrier after 300 years. The mineral saturation index (SI) was much less than zero due to the low aqueous concentration of radionuclide, so that the precipitation formation of Co-60, Sr-90, I-129, Cs-137 and Am-241 related minerals were not found. The effect of adsorption/desorption (i.e., surface complexation model) could be a crucial geochemical mechanism for the modeling of liquid-solid phase behavior of radionuclide in geochemically dynamic environments. Moreover, the development of advanced numerical models that are coupled with hydrogeochemical transport and dose assessment of radionuclide is required in the future.

INTRODUCTION

There are three nuclear power plants with six existing nuclear power units which consist of four boiling water reactors (BWR) and two pressurized water reactors (PWR) in Taiwan. These nuclear power plants are operated by the government-owned utility of Taiwan Power Company (TPC) and provide a total installed capacity of 5.144 GWe which contribute about 18% of the total electricity in Taiwan. Additionally, the 4th nuclear power plant with the design type of two advanced boiling water reactors (ABWR) is

expected to commercial operation in 2016. The total volume of low-level radioactive waste (LLW) is about 200,000 cubic meters, which is generated mainly from nuclear power plants (90-95%) and a small proportion from isotope applications (e.g., medical, industrial, and educational activities). LLW is currently stored in nuclear power plants and at Lanyu Storage Site in Lanyu Island temporarily. The site selection for LLW disposal is a challenging task. The general concerns are the hydrological and hydrogeological site conditions. One of potential sites located at a Dongjiyu islet of Penghu County in the middle line of Taiwan Strait was proposed in 2008. However, disputations and political wrangling forced the county government to delineate the Dongjiyu islet as a Nature Reservation Area in 2009 and the siting process was aborted. In 2011, two potential sites, Daren and Wuchiu islet, have been again on the selected list by Taiwan Power Company for final disposal of LLW located in the southeastern coast of Taiwan island and Taiwan's offshore island near the mainland China, respectively. The Daren site could become a final disposal repository of LLW in Taiwan.

Several current LLW disposal concepts indicate that solidification or immobilization and packaging of wastes are normally carried out to enhance the safety of the disposal system [1-3]. The engineered barriers system (EBS) is an integral part of the radioactive waste disposal facility. The EBS represents the manmade, engineered materials of a repository, including the waste form, waste canisters, concrete barrier, buffer materials, backfill, and seals which can be used as physical and/or chemical obstructions to prevent or retard the migration of radionuclides [1]. Over the past few decades, a number of studies focused on the assessment of EBS with the properties of encapsulation, isolation, or retardation of a variety of nuclear hazardous contaminants to ensure the reliable long-term performance of such a disposal concept. There have been many successful examples of repository development, but also of failures in repository performance. Examples of such failures include the rapid leaching of radionuclides from some wastes and radionuclide releases due to the flooding of disposal trenches by rainwater or a rising water table (bathtubbing). These past failures were caused by inadequate characterization of the site, unsatisfactory performance of engineered barriers and inadequate control of the nature and inventory of long-lived radionuclides and other toxic waste emplaced in the repository. [3]

The function of the EBS is to prevent and/or hinder the release of radionuclides from the waste to the host rock and biosphere. However, the repository environment (e.g., pH, Eh, and ionic composition of the surrounding water) affects EBS performance in waste storage and disposal. Therefore, quantitative prediction of radionuclide transport in EBS is critical to evaluate the risks associated with radionuclide releasing. In the past, groundwater and radionuclide transport calculations for performances assessment of a LLW often asked empirical approaches such as the linear isotherm (Kd approach) to handle the heterogeneous interphase reactions [4-7]. A distribution coefficient (Kd) can describe the heterogeneous interphase behavior of radionuclide on a particular solid phase at a specific pH, Eh, and ionic composition of the surrounding water, but under variable environmental conditions the Kd approach cannot predict the behavior of radionuclide in geochemically dynamic environments. Surface complexation model can

account for changes in ionic composition of water chemistry and mineralogy as a function of time and their effects on radionuclide geochemical transport [8]. Reactive chemical transport model incorporates the surface complexation reactions can provide a much more powerful basis for assessing the radionuclide reactive transport through the EBS.

Therefore, the present study aims to compile the thermodynamic equilibria data among cementitious media, radionuclides (e.g., Co-60, Sr-90, I-129, Cs-137 and Am-241) and minerals of bentonite, and incorporate with reactive chemical transport model for assessing the hydrogeochemical transport of radionuclides through EBS. The results of this study will answer various questions of long-term behavior of radionuclides migration in the proposed sites. Moreover, this study provides a detailed picture of the long-term evolution of the hydrogeochemical environment and radionuclides transport of the proposed LLW disposal sites in Taiwan.

STUDY AREA

A proposed site for the final disposal of LLW is located in the Daren Township of Taitung County along the southeastern coast of Taiwan. The geology of the Daren site consists of argillite and meta-sedimentary rocks. A mined cavern design with a tunnel system of 500 m below the surface is proposed [9]. Concrete is used as the confinement material for the engineered barrier. Concrete is mainly composed of a mixture of cement, water, and aggregates. The aggregates consist of minerals such as sand, gravel, and stone, which are chemically inert to water and concrete solid. The mineral compounds in cement are calcium silicates(Ca_3SiO_5 and Ca_2SiO_4), aluminate ($Ca_3Al_2O_6$), and ferrite ($4CaO \cdot Al_2O_3 \cdot Fe_2O_3$), abbreviated as C3S, C2S, C3A, and C4AF. When these constituents are mixed with water, calcium-silicate-hydrate (C-S-H), portlandite ($Ca(OH)_2(s)$), ettringite (Aft), monosulfate (AFm), and hydrogarnet form in the cement hydration process. These hydration products also control the setting and hardening of the concrete. These alterations have direct consequences on the engineering properties of the concrete barrier. Figure 1 schematically illustrates the design of an engineered barrier in the proposed Daren site. The thickness of the concrete barrier ranges from 0.5 m to 1.0 m. The inner and outer thicknesses of the bentonite buffer are 0.5 m and 0.2 m, respectively. The chemical composition of Taiwan Cement and the calculated amount of the clinker phases in the unhydrated cement that was used in this study are listed in Table I. The mixed proportion of concrete components and their physical properties are summarized in Table II.

NUMERICAL MODELS

The groundwater quality data was limited because a groundwater monitoring network was not set up yet in the Daren site. Therefore, a thermodynamic equilibrium model, PHREEQCI [10], was used to determine the equilibrium composition of the pore water as groundwater reacting with geological mineral of argillite. The PHREEQCI is a complete windows-based graphical user interface version of the geochemical computer program PHREEQC [11], which was developed by the U.S. Geological Survey, and provides all

of the capabilities of the geochemical model PHREEQC, including speciation, batch-reaction, 1D reactive-transport, and inverse modeling. The calculated results were used to represent the groundwater quality of the Daren site in this study.

(A)

(B)
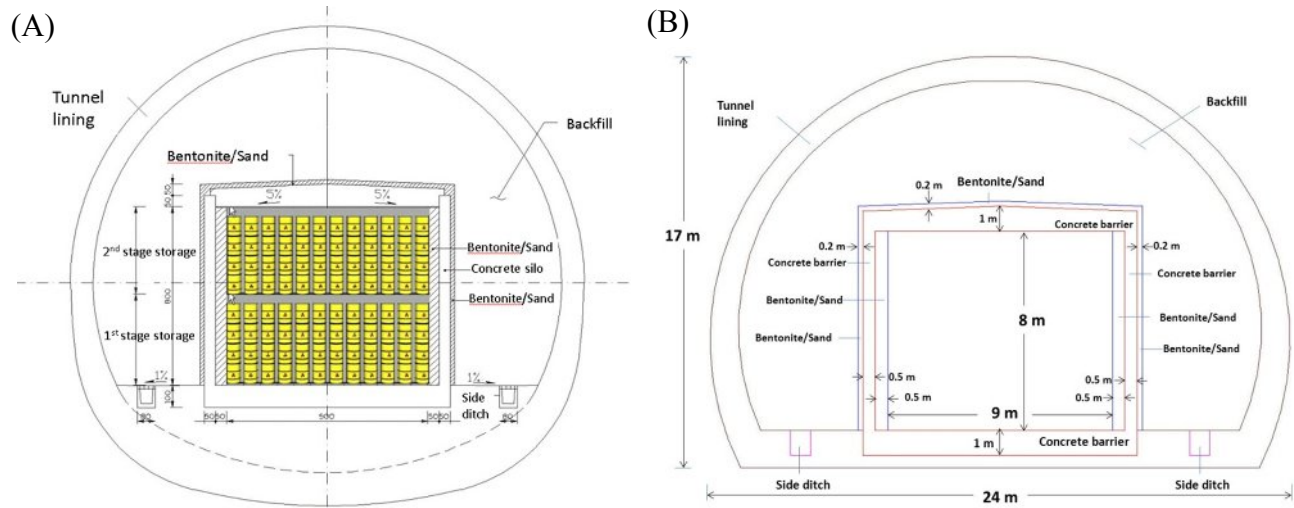
Fig 1. Schematic illustration of the EBS design in the Daren site: (A) Cross-section of the tunnel (B) Conceptual model for the cross-section of the tunnel.

Table I Chemical composition and corresponding clinker phases in Taiwan Cement.

Component	Content % by weight
CaO	61.96
SiO_2	20.42
Al_2O_3	4.95
Fe_2O_3	3.09
MgO	3.29
$Na_2O+0.685K_2O$	Max. 0.6
SO_3	2.4
Corresponding clinker component	
Tricalcium silicate (C_3S)	49
Dicalcium silicate (C_2S)	21
Tricalcium aluminate (C_3A)	7.9
Tetracalcium aluminate ferrite (C_4AF)	9.4
Abbreviations used as following: C=CaO, S=SiO_2, A=Al_2O_3, F=Fe_2O_3, H=H_2O	

Table II   Mixed proportion of concrete components and their physical properties.

Component	Content % by Volume
Cement +Water	30
Ballast	70
Physical Properties	**Parameter**
Density	2030kg/m^3
w/c ratio	0.5
Porosity	0.15

To evaluate the hydrogeochemical transport of radionuclides through EBS in the near field, a multi-species coupled geochemical transport model HYDROGEOCHEM5.0 [12] was used to simulate the reactive chemical transport processes that are involved in the long-term behavior of radionuclides migration. The computer program HYDROGEOCHEM 5.0, developed by Yeh et al. [12], is a 3-D numerical model of fluid flow, thermal, hydrologic transport, and biogeochemical kinetic and equilibrium reactions in saturated and unsaturated media. HYDROGEOCHEM 5.0 was designed for generic applications to reactive transport problems that are controlled by both kinetic and equilibrium reactions in subsurface media. The effect of precipitation and dissolution on the change of pore size, hydraulic conductivity, and diffusion/dispersion were also incorporated. The flow equations, chemical transport equations, chemical equilibrium equations, initial boundary conditions, and numerical methods of the model are described in HYDROGEOCHEM 5.0 manual [12].

HYDROGEOCHEMICAL TRANSPORT OF RADIONUCLIDES

The safety-concerned radionuclides, Co-60, Sr-90, Cs-137, I-129 and Am-241, were selected in the simulation of hydrogeochemical transport. Each radionuclide anticipated activity of operating and decommissioning LLW contained in about 998,000 fifty-gallon drums are shown in Table III. In order to quantitative prediction of radionuclide behavior in reactive transport modeling of HYDROGEOCHEM5.0, the unit conversion from the activity of radionuclides to molar concentration of aqueous radionuclide is given by Equation 1 with an assumption of saturated solidified waste and porosity of 0.15 in the cement-solidified waste form as shown in Table III.

$$A = \frac{\lambda M N^0}{W}$$

(Eq. 1)

where A is activity (Bq); λ is decay constant; M is mass of radionuclide; N^0 is Avogadro`s number (6.02×10^{23}); W is gram atomic weight.

Table III   The half-life and activity for the safety- concerned radionuclides.

Radionuclide	Half-life (years)	Activity (Bq)	Concentration (mole/l)
Co-60	5.27	1.62×10^{13}	6.58×10^{-15}
Sr-90	28.78	1.12×10^{13}	2.49×10^{-14}
I-129	1.57×10^{7}	4.48×10^{11}	5.42×10^{-10}
Cs-137	30	1.65×10^{14}	3.82×10^{-13}
Am-241	432	9.66×10^{11}	3.21×10^{-14}

The simulation region with an elevation of 40 m at the bottom was discretized with 3,918 elements and 4,146 nodes. The grid comprised cells of dimensions Δx, the Δy varied from 1m to 0.1 m, and $\Delta z=2$ m, as illustrated in Figure 2.   Model simulation time is 300 years with initial time-step of 1.0×10^{-5} year, and maximum allowable time-step of 0.01 year. The vertical front edge, back edge, and horizontal top edge depict a no-flow boundary, except for the side ditch in the vertical front edge. The side ditch area on the front edge was set to a variable boundary condition, which is usually an air-media interface in which water uninterruptedly seeps out. The flux in the bottom edge caused by gravity was considered a Neumann boundary with a zero flux. The horizontal left and right edges were Dirichlet head-boundary conditions. This hydraulic head value of Dirichlet boundary was estimated from the steady-state simulated groundwater flow (that is, $Vx=4.0 \times 10^{-8}$ m/s, to left; $Vz=3.3 \times 10^{-8}$ m/s, downward) in the proposed site of Arnold [13]. The estimated total head on the horizontal left and right edge nodes were assumed as 420 dm and 432.8 dm, respectively.
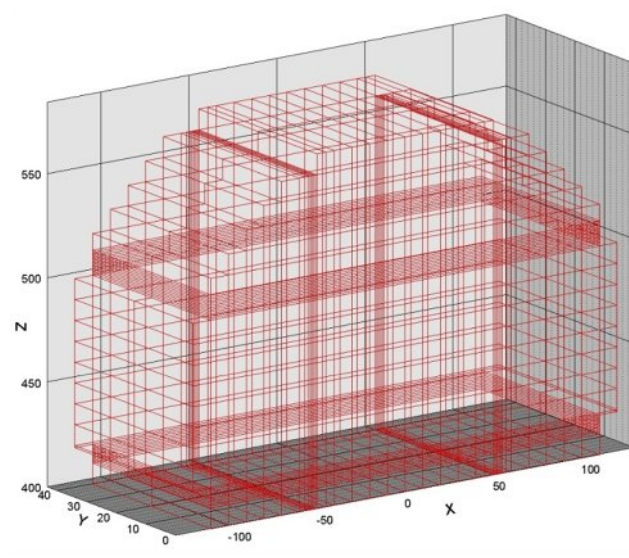
Fig 2.   The numerical discretization of grids for HYDROGEOCHEM 5.0.

Table IV Rain water quality used in the thermodynamic equilibrium model.

Species	Cl^-	SO_4^{2-}	Na^+	K^+	Ca^{2+}	Mg^{2+}	pH
Concentration (Units:µmol/l)	158.2	59.5	84.8	64.5	19	25.3	5.2

As groundwater monitoring wells have not yet been set up in the proposed site, the groundwater quality data are very limited. Therefore, a thermodynamic equilibrium model, the PHREEQCI was first used to calculate the porewater composition that equilibrated with rainwater (see Table IV), groundwater, and geological mineral of argillite (that is, montmorillonite, calcite, chlorite, dolomite, illite, feldspar, mica, kaolinite, pyrite, quartz, and siderite). The calculated results represented groundwater quality of the proposed site in this study. Table V provides a summary of the physical parameters for groundwater flow and the reactive transport simulations. Table VI presents the initial and boundary conditions, and other parameters that were used in reactive chemical transport modeling. The study considered the hydrogeochemical transport of 11 components, including Na^+, K^+, Ca^{2+}, Al^{3+}, OH^-, HCO_3^-, Cl^-, SO_4^{2-}, H_4SiO_4, Fe^{3+}, e^-, Co^{2+}, Sr^{2+}, Cs^+, Am^{3+}, I^-, 51 aqueous species, 13 solid-phase radionuclides of precipitation/dissolution reactions, 10 minerals of precipitation/dissolution reactions, and 4 adsorbed species. Table VII-X list the thermodynamic data of reactions (e.g,: precipitation-dissolution, adsorption-desorption, and aqueous complexation) considered in the HYDROGEOCHEM 5.0. The surface complexation model (e.g., constant capacitance model) is used to describe sorption of cesium on the silica surface of cement mineral. The adsorbent component, SOH, is specified as a sorbing site of silica surface. The model simulation time was 300 years with an initial time-step of 1.0×10^{-5} year, and a maximal allowable time-step of 0.01 year. In addition, the precipitation/dissolution on the change of porosity, hydraulic conductivity, and hydrodynamic dispersion of cementitious media may be a crucial hydrogeochemical mechanism in the concrete degradation of EBS. Thus, the effect of precipitation/dissolution reactions on both the flow and the reactive transport were also considered in the simulations. Moreover, pyrite oxidation and sulfate reduction reactions were incorporated in the simulation scenarios on the formations of cement degradation materials.

SIMULATION CASES

Two cases of reactive transport simulations are as follows.
Case 1: Modeling the hydrogeochemical transport of radionuclides without adsorption-desorption processes
Case 2: Modeling hydrogeochemical transport of radionuclide with adsorption-desorption processes
The simulations of cases 1 and 2 were conducted by using HYDROGEOCHEM 5.0. In case 1, radionuclides of Co-60, Sr-90, Cs-137, I-129 and Am-241 were selected with only considering precipitation-dissolution in liquid-solid phase of radionuclides. In case 2, to show the effects of adsorption-desorption on the geochemical transport, adsorption-desorption reaction of Cs-137 was

included in the radionuclide transport modeling.

Table V Physical parameters used in HYDROGEOCHEM 5.0 model.

Media	K (m/s)	Porosity (%)	Diffusion coefficient (m^2/s)	Bulk density (kg/m^3)	Longitudinal dispersivity (m)	Lateral dispersivity (m)
Cement-solidified waste canister	8.70×10^{-9}	0.15	3.0×10^{-12}	1200	0.1	0.01
Concrete	3.1×10^{-14}	0.15	3.0×10^{-12}	2030	0.10	0.010
Bentonite	5.0×10^{-11}	0.363	1.2×10^{-10}	2000	0.15	0.015
Backfill	3.24×10^{-8}	0.168	2.0×10^{-11}	2410	0.30	0.030

Table VI Initial and boundary conditions of component concentration (mole/l) used in HYDROGEOCHEM 5.0 model.

Component	Initial Conditions				Boundary Conditions
	Concrete	Bentonite	Backfill	Cement-solidified waste form	Groundwater
Na^+	6.908×10^{-2}	1.69×10^{-1}	1.01×10^{-4}	1.50×10^{-2}	7.68×10^{-5}
K^+	0.2665	1.14×10^{-3}	1.84×10^{-6}	8.90×10^{-2}	1.84×10^{-6}
Ca^{2+}	29.906	9.97×10^{-3}	3.61×10^{-2}	15.46	3.21×10^{-2}
Al^{3+}	2.628	1.00×10^{-20}	3.33×10^{-14}	5.16×10^{-1}	2.71×10^{-8}
OH^-	21.1	1.91×10^{-7}	3.43×10^{-7}	7.75	3.43×10^{-7}
HCO_3^-	1.394×10^{-11}	2.14×10^{-3}	3.60×10^{-4}	1.22×10^{-1}	3.81×10^{-4}
Cl^-	5.64×10^{-5}	1.53×10^{-1}	1.79×10^{-4}	3.80×10^{-2}	1.58×10^{-4}
SO_4^{2-}	1.633×10^{-3}	2.94×10^{-2}	8.57×10^{-2}	1.633×10^{-3}	8.81×10^{-2}
H_4SiO_4	9.198	6.60×10^{-5}	1.51×10^{-4}	4.72×10^{0}	1.51×10^{-4}
Fe^{3+}	3.10×10^{-2}	1.0×10^{-8}	1.0×10^{-10}	3.1×10^{-2}	8.79×10^{-4}
pe	-1.0	-0.70	-1.0	-1.0	-1.0

Table VII Precipitation-dissolution reactions of solid-phase radionuclides considered in the HYDROGEOCHEM 5.0 model.

	Precipitation-dissolution reactions of solid-phase radionuclides (25℃)				
No.	Reaction	log K	No.	Reaction	log K
1	$Co^{2+}+2OH^-=Co(OH)_{2(S)}$	15.70	8	$2Cs^++2OH^-=Cs_2O_{(S)}+H_2O$	-96.43
2	$Co^{2+}+CO_3^{2-}=CoCO_{3(S)}$	10.00	9	$Co^{2+}+2I^-+12OH^-=Co(IO_3)_{2(S)}+12e^-+6\,H_2O$	-47.22
3	$Co^{2+}+3OH^-=Co(OH)_{3(S)}+e^-$	12.47	10	$Sr^{2+}+2I^-+12OH^-=Sr(IO_3)_{2(S)}+12e^-+6\,H_2O$	-44.74
4	$3Co^{2+}+8OH^-=Co_3O_{4(S)}+2e^-$	49.12	11	$Ca^{2+}+2I^-+12OH^-=Ca(IO_3)_{2(S)}+12e^-+6\,H_2O$	-45.07
5	$SiO_{2(aq)}+Sr^{2+}+2OH^-=SrSiO_{3(S)}+H_2O$	13.92	12	$Am^{3+}+3OH^-=Am(OH)_{3(S)}$	26.4
6	$Sr^{2+}+CO_3^{2-}=SrCO_{3(S)}$	9.00	13	$Am^{3+}+3I^-=AmI_{3(s)}$	25.3
7	$Sr^{2+}+SO_4^{2-}=SrSO_{4(S)}$	6.50			

Table VIII Precipitation-dissolution reactions of cement mineral considered in the HYDROGEOCHEM 5.0 model.

No.	Mineral	Reaction	log K	Molar volume (dm^3/mole)
		Precipitation-dissolution reactions of cement mineral (25℃)		
1	Calcite	$HCO_3^- + Ca^{2+} + OH- = CaCO_3 + H2O$	12.151	0.03693
2	Portlandite	$Ca^{2+} + 2OH- = Ca(OH)_2$	5.20	0.03300
3	Ettringite	$2Al^{3+} + 6Ca^{2+} + 26H_2O + 3SO_4^{2-} +12OH- = Ca_6Al_2(SO_4)_3(OH)_{12}·26H_2O$	111.03	0.71032
4	Quartz	$H4SiO4 = SiO2 + 2H2O$	3.98	0.02269
5	Gypsum	$Ca^{2+} + SO4^{2-} + 2H2O = CaSO4·2H2O$	4.58	0.07470
6	Hydrogarnet	$2Al^{3+} + 3Ca^{2+} + 12OH- = Ca_3Al_2(OH)_{12}$	87.68	0.14952
7	Friedel's salt	$2Al^{3+} + 4Ca^{2+} + 2Cl^- + 4H_2O + 12OH- = 2Ca_2Al(OH)_6Cl·2H_2O$	93.07	0.27624
8	Thaumasite	$3Ca^{2+}+H_4SiO_4+SO_4^{2-}+HCO_3^-+11H_2O +3OH^-=CaSiO_3·CaSO_4·CaCO_3·15H_2O$	31.70	0.32940
9	Monocarboaluminate	$2Al^{2+} +HCO_3^- + 4Ca^{2+} + 3.68H_2O + 13OH- = 3CaO·Al_2O_3·CaCO_3·10.68H_2O$	101.45	0.26196
10	Pyrite	$FeS_2 + 2H^+ + 2e^- = Fe^{+2} + 2HS^-$	-18.479	0.02394

Table IX   Adsorption-desorption reactions considered in the HYDROGEOCHEM 5.0 model.

No.	Reaction	log K	No.	Reaction	log K
	Adsorption-Desorption Reactions (25℃)				
1	$SO- + H^+ = SOH$	7.6	3	$SOH + Cs^+ = SOCs + H^+$	-5.5
2	$SOH + Cs^+ = SOHCs^+$	2.05	4	$SOH + Na^+ = SOHNa^+$	2.0

Table X   Aqueous complexation reactions considered in the HYDROGEOCHEM 5.0 model.

No.	Reaction	log K	No.	Reaction	log K
	Aqueous complexation reactions (25℃)				
1	$HCO_3^- = CO_{2(aq)} + OH^-$	-7.648	27	$Na^+ + Cl^- = NaCl$	-0.5
2	$HCO_3^- + 8e^- + 6H_2O= CH_{4(aq)} + 9OH^-$	-95.258	28	$Na^+ + HCO_3^- + OH^- = NaCO_3^- + H_2O$	4.961
3	$4OH^- = O_2 +2H_2O +4e^-$	-30.08	29	$Na^+ + OH^- = NaOH$	-0.18
4	$2H_2O + 2e^- = 2OH^- + H_2$	-31.15	30	$Na^+ + SO_4^{2-} = NaSO_4^-$	0.94
5	$H_2O = OH^- + H^+$	-14	31	$SO_4^{2-} + H_2O = HSO_4^- + OH^-$	-12.012
6	$Al^{3+}+OH^- +H_4SiO_4=AlH_3SiO_4^{2+}+H_2O$	-16.38	32	$SO_4^{2-} + 8e^- + 4H_2O = S^{2-} + 8OH^-$	-91.268
7	$H_4SiO_4+2OH^-=H_2SiO_4^{2-}+2H_2O$	5	33	$SO_4^{2-} + 8e^- + 5H_2O = HS^- + 9OH^-$	-92.35
8	$Ca^{2+}+H_4SiO_4+OH^-=CaH_3SiO_4^++H_2O$	5.17	34	$SO_4^{-2} + 6H_2O + 8e^- = H_2S + 10OH^-$	-99.356
9	$Mg^{2+}+H_4SiO_4+OH^-=MgH_3SiO_4^++H_2O$	5.42	35	$FeCO_3 = Fe^{3+} + HS^- + e^-$	-23.82
10	$H_4SiO_4 + OH^- = H_3SiO_4^- + H_2O$	4.17	36	$Co^{2+} + OH^- = CoOH^+$	4.30
11	$Na^++H_4SiO_4+OH^-=NaH_3SiO_{4(aq)}+H_2O$	5.99	37	$Co^{2+} + 2OH^- = Co(OH)_2$	9.20
12	$Al^{3+} + 4OH^- = Al(OH)_4^-$	33.3	38	$Co^{2+} + 3OH^- = Co(OH)_3^-$	10.50
13	$K^+ + Al^{3+} + 4OH^- = KAl(OH)_4$	31.78	39	$Co^{2+} + Cl^- = CoCl^+$	0.50
14	$Na^+ + Al^{3+} + 4OH^- = NaAl(OH)_4$	32.37	40	$Co^{2+} + SO_4^{2-} = CoSO_4$	2.40
15	$Ca^{2+} + Cl^- = CaCl^+$	-0.29	41	$Sr^{2+} + OH^- = Sr(OH)^+$	0.71
16	$Ca^{2+} + HCO_3^- + OH^- = CaCO_3 + H_2O$	6.895	42	$Sr^{2+} + HCO_3^- + OH^- = Sr(CO_3) + H_2O$	-0.86
17	$Ca^{2+} + OH^- = CaOH^+$	1.22	43	$Sr^{2+} + SO_4^{2-} = Sr(SO_4)$	2.3
18	$Ca^{2+} + SO_4^{2-} = CaSO_4$	2.3	44	$Am^{3+} + 2OH^- = Am(OH)_2^-$	12.9
19	$HCO_3^- + OH^- = CO_3^{2-} + H_2O$	3.671	45	$Am^{3+} + SO_4^{2-} = Am(SO_4)^+$	3.3
20	$Fe^{3+} + e^- = Fe^{2+}$	13.02	46	$Am^{3+} + Cl^- = AmCl^{2+}$	0.24
21	$Fe^{3+} + 4OH^- = Fe(OH)_4^-$	34.4	47	$Cs^+ + OH^- = Cs(OH)$	1.61
22	$K^+ + Cl^- = KCl$	-0.5	48	$Ca^{+2} + I^- = CaI^+$	0.14
23	$K^+ + OH^- = KOH$	-0.46	49	$Cs^+ + I^- = CsI$	1.05
24	$K^+ + SO_4^{2-} = KSO_4^-$	0.85	50	$Sr^{+2} + I^- = SrI^+$	0.14
25	$Mg^{2+}+HCO_3^-+OH^-=MgCO_3^++H_2O$	6.651	51	$Sr^{+2} + 2I^- = SrI_2^+$	-0.04
26	$Mg^{2+} + OH^- = MgOH^+$	2.56			

RESULT AND DISCUSSION

The simulated results revealed notable differences of flow velocity distribution in the hydrogeochemical transport of EBS. The groundwater velocity was approximately equal to zero in the concrete barrier and cement-solidified waste canister. The highest groundwater velocity occurred at the right side of ditch was over 50 times higher than the lowest groundwater velocity in the backfill materials. Thus, high groundwater inflow velocity was developed and then drained out to the side ditch. The EBS with the side ditch efficiently drained the ground water and lowered the concentration of the concrete degradation induced species (e.g., hydrogen ion, sulfate, and chloride). Figure 3 illustrated the velocity distribution of cases 1, 2, and 3. The maximal velocity of groundwater flowed on the right hand side of ditch was 8.25 dm/year and 5.88 dm/year in initial stage and after 300 years, respectively. However, the velocity of groundwater observed at side ditch gradually decreased as the simulation progresses. The precipitations of ettringite and thaumasite minerals were observed at the side ditch after 300 years as shown in Figure 4. The fouling of pore space caused by the mineral formation of ettringite and thaumasite reduced the porosity and decreased the hydraulic conductivity and groundwater velocity in the side ditch.
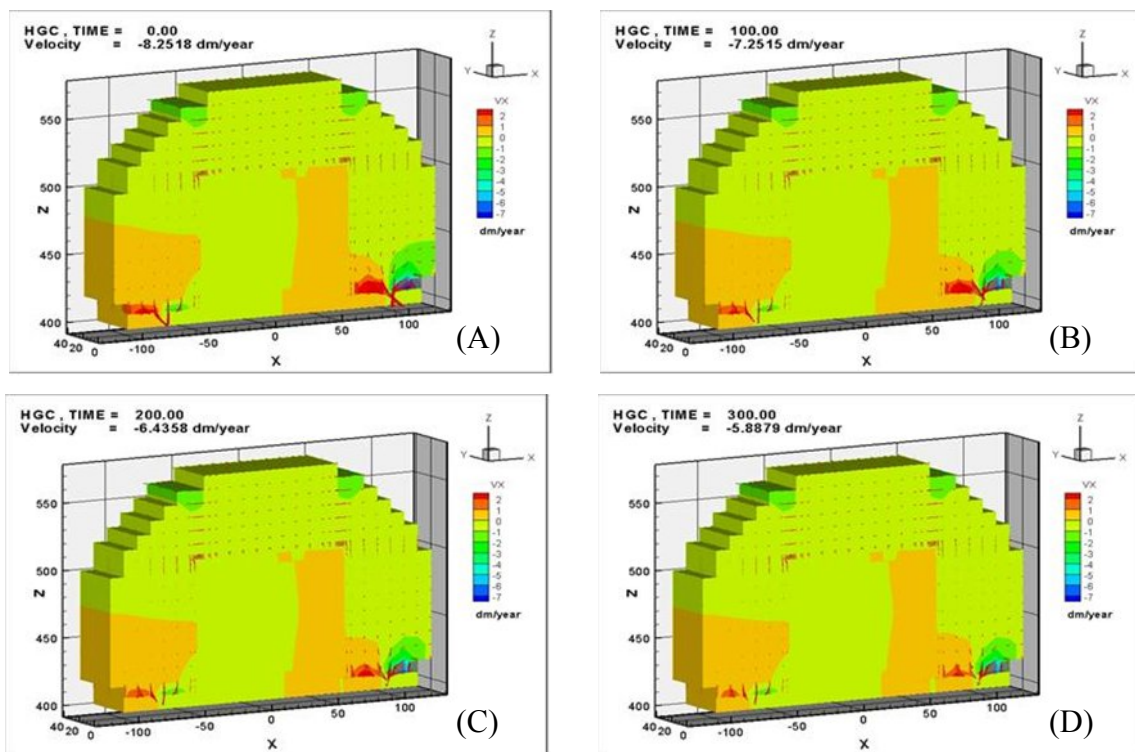
Fig 3. Velocity distribution in 0, 100, 200, and 300 years for case 1 and case 2: (A) 0 year (B) 100 years (C) 200 years (D)300 years.
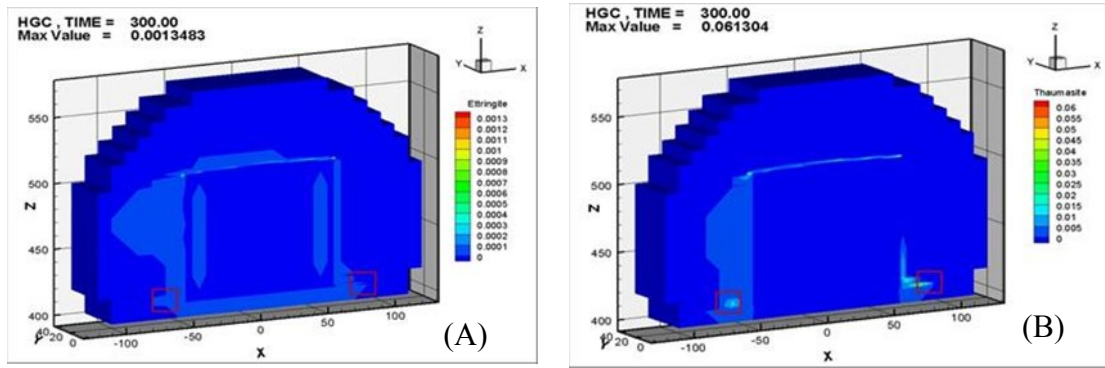
Fig 4. Distribution of ettringite and thaumasite after 300 years: (A) ettringite (B) thaumasite.
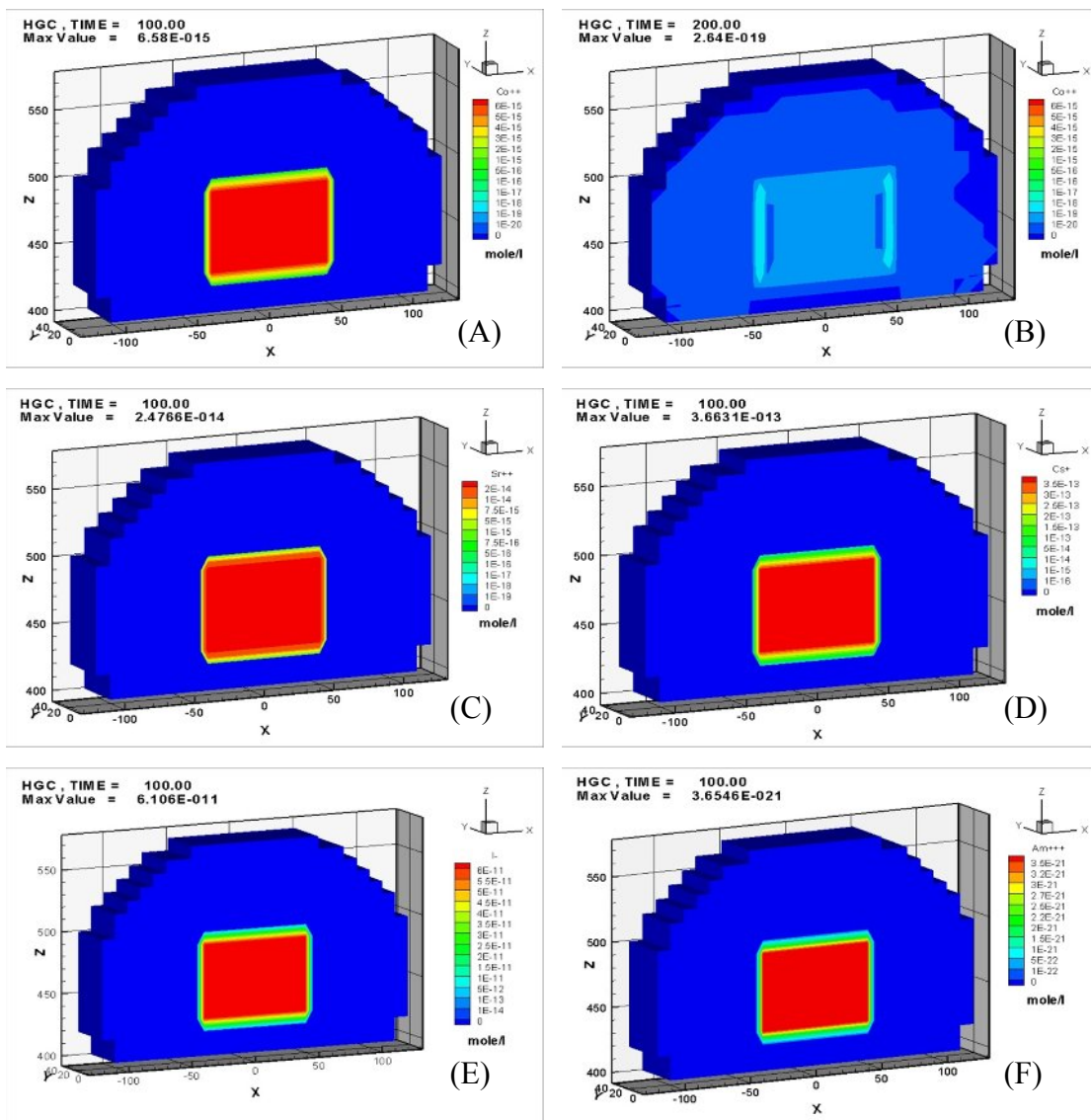
Fig 5 Distribution of radionuclides in case 1: (A) Co-60 after 100 years, (B) Co-60 after 200 years, (C) Sr-90 after 100 years, (D) Cs-137 after 100 years, (E) I-129 after 100 years, (F) Am-241 after 100 years.

In case 1, the maximal dissolved concentrations from the release of Co^{2+}, Sr^{2+}, Cs^+, I^- and Am^{3+} in the EBS were approximately 3.0×10^{-15}, 7.5×10^{-15}, 2.5×10^{-13}, 4.0×10^{-11} and 2.7×10^{-21} M after 100 years, respectively(see Figure 5). Because of the short half-life of Co-60 of 5.27 years, the concentration of Co^{2+} decreased to the amount of 2.64×10^{-19} M at the interface of waste canister and concrete barrier after 200 years, thus the concentration quickly became nil as the simulation proceeds. Similar results were also found in Sr^{2+} and Cs^+. The concentration of Sr^{2+} and Cs^+ deceased to the amount of 2.58×10^{-16} M and 5.31×10^{-15} M respectively at the interface of waste canister and concrete barrier after 300 years. The release concentration of Sr-90 and Cs-137 in the backfill materials after 300 years was approximately to 1.00×10^{-17} M and 1.00×10^{-16} M, respectively. The half-life of I-129 and Am-241 was 1.57×10^7 years and 432 years, respectively, so that the concentrations of the two radionuclides do not largely vary in the simulation and remain unchanged at the interface of waste canister and concrete barrier after 300 years. The release concentration of I-129 and Am-241 in the backfill materials after 300 years was approximately equal to 1.00×10^{-13} M and 1.00×10^{-22} M, respectively.

In case 1, the mineral saturation index (SI) was much less than zero due to the low aqueous concentrations of radionuclides, so the precipitation of Co-60, Sr-90, Cs-137 I-129, and Am-241 related minerals were not found in EBS. In case 2, however, the Cs-137 was encapsulated in the EBS. The release of concentration of dissolve Cs^+ was much less than that of in case 1. Therefore, the effect of adsorption/desorption (i.e., surface complexation model) could be a crucial geochemical mechanism for the modeling of liquid-solid phase behavior of radionuclide in geochemically dynamic environments. Evans [14] discussed the binding mechanisms of radionuclides to cement. He showed that several processes can affect the concentration of radionuclide in cement porewater, for example, precipitation as a simple salt, coprecipitation with other phases, lattice incorporation in the major cement hydration products (solid solution), sorption at hydrous surfaces (chemisorption, adsorption), and complex and colloid formation in the aqueous phase. Marmier [15] indicated that cesium can bind on the silica surface. He also demonstrated that a surface complexation model can describe sorption of cesium on the silica surface. BarNes et al. [16] also reported that cesium tends to concentrate inside agglomerated silica particles of cement. Iwaida et al. [17] observed that cesium can be sorbed on the silicate chains in C-S-H of cement. Apart from cesium, Wang et al. [18, 19] indicated that sorption of radionuclides is an important issue at water-solid interfaces in radioactive waste assessment. They developed a surface complexation model based on the diffuse-layer theory to assess the adsorption of radionuclide cations (e.g., Am^{3+}, Pu^{4+}, Pu^{5+}, and Np^{5+}) and anions (e.g., I^-, IO_3^-, SeO_3^{2-}, SeO_4^{2-}, and TcO_4^-) on various minerals. Tits et al. [20] investigated that strontium was uptake by C-S-H phases in terms of a Sr^{2+}-Ca^{2+} ion exchange model. He also showed that the selectivity coefficient for the Sr^{2+}-Ca^{2+} exchange was 1.2±0.3. These thermodynamic data allow the reactive transport model to evaluate the composition and concentration of the radionuclide solid-water interface under different hydrogeochemical environment. Bradbury et al. [21] reported the surface complexation approach to model radionuclide sorption in natural systems. They indicated that the

consequence of the empirical methodology such as distribution coefficients and isotherm equations is only valid under the experimental measured conditions, and extrapolation to other conditions and systems may be questionable. Bradbury et al. also investigated that surface complexation mechanism (e.g., diffuse layer model) was used to describe radionuclide sorption on igneous rock forming mineral. They suggested that trying to understand sorption via mechanisms, the development of model concepts, and the use of predictive models is the only feasible approach which has the potential to provide defensible sorption values in safety assessment studies over the wide range of conditions required [21]. Therefore, Adsorption/desorption reactions (i.e., surface complexation model) can attenuate in hydrogeochemical transport of radionuclides through EBS.

A performance assessment methodology not only requires the ability to simulate the potential source-term release and far-field transport of the concerned radionuclides, but must also consider the potential exposure pathways of the radionuclides to a near-by resident of which the accompanying dose that these individuals might incur [13]. Therefore, in the safety assessment for the LLW disposal, evaluation of ecological and health risks should be included in the model. Integration of hydrogeochemical transport module and dose assessment code, such as the HYDROGEOCHEM code and RESRAD family of codes [22] is imperative. The developed tool can provide confidence in the protectiveness of the human and environmental health for safety assessment of the EBS in the near field.

CONCLUSION AND SUGGESTION

HYDROGEOCHEM5.0 model was applied to simulate the complex chemical interactions among radionuclides, the cement minerals of the concrete, groundwater flow, and transport in the proposed site. The simulation results revealed that the EBS with the side ditch efficiently drained the ground water and lowered the concentration of the concrete degradation induced species (e.g., hydrogen ion, sulfate, and chloride). The velocity of groundwater observed at side ditch gradually decreased as the simulation proceeds. Ettringite and thaumasite minerals were observed at the side ditch after 300 years. The fouling of pore space caused by the precipitation can induce the porosity reduction and result in the decrease of hydraulic conductivity and groundwater velocity in side ditch. Due to short half-life of Co-60, Sr-90 and Cs-137, the concentration of these radionuclides decreased soon as the simulation progress. The long half-life of I-129(1.57×10^7 years) and Am-241(432 years) remain stable concentrations at the interface of waste canister and concrete barrier after 300 years. The mineral saturation index (SI) was much less than zero due to the low aqueous concentration of radionuclides, thus the formation of Co-60, Sr-90, I-129, Cs-137 and Am-241 related minerals were not found in EBS. This will lead us further into the consideration of adsorption/desorption (i.e., surface complexation model) which could be a crucial geochemical mechanism for the modeling of liquid-solid phase behavior of radionuclide in geochemically varied environments. Furthermore, the development of advanced numerical models that are coupled with hydrogeochemical transport and dose assessment of radionuclide is required in future research. The

effective prediction tool of the advanced numerical models can provide confidence in the protection of the human and environmental health for performance assessment of the EBS.

ACKNOWLEGEMENT

REFERENCES

1. IAEA. (2001). Performance of Engineered Barrier Materials in Near Surface Disposal Facilities for Radioactive Waste, p.50, IAEA — TECDOC-1255, Vienna.

2. IAEA. (2001). Technical considerations in the design of near surface disposal facilities for radioactive waste, p.53, IAEA — TECDOC-1256, Vienna.

3. IAEA. (1999). Near Surface Disposal of Radioactive Waste, IAEA Safety Standards Series, Requirements, p.29, IAEA —WS-R-1, Vienna.

4. Ochs, M., Pointeau, I., and Giffaut, E. (2006). Caesium sorption by hydrated cement as a function of degradation state: experiments and modelling. *Waste Management*, 26, 725-732.

5. Sullivan, T.M. (1993). Disposal Unit Source Term (DUST) Data Input Guide. Technical Report NUREG/CR6041, BNL-NUREG-52375, U. S. Nuclear Regulatory Commission, Washington, DC.

6. Sullivan, T.M. and Suen, C. J. (1989). Low-Level Waste Shallow Land Disposal Source Term Model: Data Input Guides, Technical Report NUREG/CR-5387, BNL-NUREG-52206, U. S. Nuclear Regulatory Commission, Washington, DC.

7. Kozak, M.W., Chu, M S.Y., Mattingly, P.A., Johnson, J. D., and McCord, J. T. (1990). Background Information for the Development of a Low-Level Waste Performance Assessment Methodology - Computer Code Implementation and Assessment, Technical Report NUREG/CR-5453, SAND90-0375, Vol. 5, U. S. Nuclear Regulatory Commission, Washington, DC.

8. Zavarin, M. and Bruton, C. J. (2004). A Non-Electrostatic Surface Complexation Approach to Modeling Radionuclide Migration at the Nevada Test Site: Iron Oxides and Calcite. Technical Report UCRL-TR-208673, Lawrence Livermore National Laboratory, Livermore, California.

9. Taiwan Power Company. (2010). Performance assessment in low-level radioactive waste disposal facility, version B (in Chinese), p. 513, Taiwan Power Company.

10. USGS. 2011. Phreeqcl--A Graphical User Interface for the Geochemical Computer Program PHREEQC, http://wwwbrr.cr.usgs.gov/projects/GWC_coupled/phreeqci/.

11. PARKHURST, D.L. and APPELO, C.A.J. (1999). User's guide to PHREEQC (Version 2) — A Computer Program for Speciation, Batch-Reaction, One-Dimensional Transport, and Inverse Geochemical Calculations: U.S. Geological Survey Water Resources Investigations Report

99-4259, p. 310, U.S. Geological Survey, Denver, Colorado.

12. Yen, G.T., Sun, J., Jardine, P.M., Burgos, W.D., Fang, Y., Li, M.H. and Siegel, M.D. (2004). HYDROGEOCHEM 5.0: A three-Dimensional model of coupled fluid flow, thermal transport, and hydrogeochemical transport through variably saturated conditions – version 5.0, Technical Report ORNL/TM-2004/107, p. 243,Oak Ridge National Laboratory, Oak Ridge, TN.

13. Arnold, B.W., Knowlton, R.G., Schelling, F.J., Mattie, P.D., Cochran, J.C. and Jow, H.N. (2007). Taiwan Industrial Cooperation Program Technology Transfer for Low-Level Radioactive Waste Final Disposal – Phase I, p. 148, Sandia National Laboratories, SAND2007-0131, NM.

14. Evans, N. (2008). Binding mechanisms of radionuclides to cement. *Cement and Concrete Research*, 38, 543–553

15. Marmier N., Delisée, A., and Fromage, F. (1999). Surface complexation modeling of Yb(III) and Cs(I) sorption on silica. *Journal of Colloid and Interface Science*, 212, 228–233.

16. BarNes, G., Katz, A., Peled, Y., and Zeiri, Y. (2008). The mechanism of cesium immobilization in densified silica-fume blended cement pastes, *Cement and Concrete Research*, 38, 667-674.

17. Iwaida, T., Nagasaki, S., Tanaka, S., Yaita, T. (2001). Sorption of alkali metal ions onto C–S–H (calcium silicate hydrated phases), *Cement and Concrete Science & Technology*, 55**,** 21-26.

18. Wang, P., Anderko, A., and Turner, D.R. (2001). Thermodynamic modeling of the adsorption of radionuclide on selected minerals: I. Cations, *Industrial & Engineering Chemistry Research*, 40, 4428-4443.

19. Wang, P., Anderko, A., and Turner, D.R. (2001). Thermodynamic modeling of the Adsorption of Radionuclides on Selected Minerals. II: Anions, *Industrial & Engineering Chemistry Research*, 40, 4444-4455.

20. Tits, J, Wieland E, Müller C.J., Landesman D, and Bradbury M.H. (2006). Strontium binding by calcium silicate hydrates. *Journal of Colloid and Interface Science*, 300, 78-87.

21. Bradbury, M.H. and Baeyens, B. (1993). A general application of surface complexation to modeling radionuclide sorption in natural systems, *Journal of Colloid and Interface Science*, 158, 364-371.

22. Yu, C., Zielen, A.J., Cheng, J.-J., LePoire, D.J., Gnanapragasam, E., Kamboj, S., Arnish, J., Wallo III, A., Williams, W.A., and Peterson, H. (2001). *User's Manual for RESRAD Version 6*, ANL/EAD-4, Argonne National Laboratory, Argonne, IL.